

Effects of magnetism and doping on the electron-phonon coupling in BaFe_2As_2

L. Boeri,¹ M. Calandra,² I. I. Mazin,³ O.V. Dolgov,¹ and F. Mauri²

¹*Max-Planck-Institut für Festkörperforschung, Heisenbergstraße 1, D-70569 Stuttgart, Germany*

²*CNRS and Institut de Minéralogie et de Physique des Milieux Condensés,
case 115, 4 place Jussieu, 75252 Paris Cedex 05, France*

³*Naval Research Laboratory, 4555 Overlook Avenue SW, Washington, DC 20375, USA*

(Dated: April 13, 2010)

We calculate the effect of local magnetic moments on the electron-phonon coupling in $\text{BaFe}_2\text{As}_2 + \delta$ using the density functional perturbation theory. We show that the magnetism enhances the total electron-phonon coupling by $\sim 50\%$, up to $\lambda \lesssim 0.35$, still not enough to explain the high critical temperature, but strong enough to have a non-negligible effect on superconductivity, for instance, by frustrating the coupling with spin fluctuations and inducing order parameter nodes. The enhancement comes mostly from a renormalization of the electron-phonon matrix elements. We also investigate, in the rigid band approximation, the effect of doping, and find that λ versus doping does not mirror the behavior of the density of states; while the latter decreases upon electron doping, the former does not, and even increases slightly.

PACS numbers: 63-20.dk, 63-20.Kd, 74-20.Pq, 74-70.Xa

The simultaneous presence of high T_c superconductivity and magnetism in the phase diagram of the Fe-based superconductors (FBSC) suggests that magnetism plays an important role in determining the superconducting properties. Phonons have been excluded early on as possible mediators, on the basis of first-principles non-magnetic calculations for the undoped compound,^{1,2} but the experimental situation is still far from settled in this regard.³⁻⁵

Density functional (DFT) calculations correctly reproduce several properties of Fe pnictides, such as the magnetic pattern in the parent compounds and the geometry of the Fermi surface. The interplay of magnetic and elastic properties is however puzzling:⁶ on one hand, experiments measure weak magnetic moments ($m \sim 0.3 - 1.0 \mu_B$) in the SDW state and no long-range magnetic order in the superconducting samples, while spin-polarized LSDA calculations predict large magnetic moments at all dopings ($m \sim 2.0 \mu_B$). On the other hand, the same spin-polarized LSDA calculations predict equilibrium structures and phonon densities of states that are much closer to the experiment than those predicted by non-magnetic calculations.⁷⁻⁹ A possible way to reconcile these two apparently conflicting results is an itinerant picture, in which the Fe atoms nevertheless have large local magnetic moments that order below the Neel temperature in the undoped compound, but survive locally at all dopings.^{10,11} But this point of view immediately raises the question of whether the estimate of electron-phonon ($e-ph$) matrix elements given by early non-magnetic (rather than paramagnetic, *i. e.*, with the local Fe moment entirely suppressed) DFT calculations is representative of the actual compounds.¹²

In this paper, we calculate from first principles the $e-ph$ coupling constant in antiferromagnetic (AFM) and non-magnetic (NM) BaFe_2As_2 , using the linear response method.¹³ We confirm that magnetism strongly affects the phonon frequencies, leading to a renormalization of

the modes that involve Fe-As vibrations,⁷⁻⁹ and also find a strong effect on the $e-ph$ matrix elements, leading to a $\sim 50\%$ increase with respect to the NM values. Using a rigid-band model, we show that the $e-ph$ coupling constant λ as a function of doping does not follow the density of states. Finally, we estimate the $e-ph$ coupling in the *paramagnetic* (PM) state, by combining the *nonmagnetic* band structure (eigenenergies and eigenfunctions) with the *magnetic* phonon spectra and self-consistent potentials. For the relevant values of doping, we estimate an upper bound to the $e-ph$ coupling constant $\lambda = 0.35$, *i.e.* not high enough to explain superconductivity, but not sufficiently weak to be neglected. For instance, $e-ph$ interaction may be one of the factors responsible for experimentally observed gap anisotropy.

Magnetic Order	$m (\mu_B)$	$N(0)(\text{eV}^{-1})$	$\lambda_{\sigma\sigma}$	$\omega_{ln}(\text{K})$	$\lambda_{\sigma\sigma}/N(0)$
NM	0.0	1.18	0.18	194	0.15
AFMc	2.4	1.36	0.33	179	0.24
AFMs	2.6	0.68	0.18	180	0.26
PM1	*	1.18	0.27	206	0.23
PM2	*	1.18	0.27	195	0.23
PM3	*	1.18	0.31	170	0.26

TABLE I: Calculated properties of BaFe_2As_2 . m is the integral over the cell of the absolute value of the magnetization, $N(0)$ is the DOS in states/(spin eV Fe atom), $\lambda_{\sigma\sigma}$ is the electron-phonon coupling and ω_{ln} is the logarithmic-averaged phonon frequency. In addition to the three fully self-consistent calculations we report here three model calculations (see text): PM1 utilizes the wave functions, one-electron energies and phonon frequencies from the NM calculations, and the deformation potentials from the AFMc calculations. PM2 and PM3 use one-electron energies and wave functions from the NM calculations, and phonon frequencies and deformation potentials from the AFMc and AFMs calculations, respectively.

Report Documentation Page			Form Approved OMB No. 0704-0188		
Public reporting burden for the collection of information is estimated to average 1 hour per response, including the time for reviewing instructions, searching existing data sources, gathering and maintaining the data needed, and completing and reviewing the collection of information. Send comments regarding this burden estimate or any other aspect of this collection of information, including suggestions for reducing this burden, to Washington Headquarters Services, Directorate for Information Operations and Reports, 1215 Jefferson Davis Highway, Suite 1204, Arlington VA 22202-4302. Respondents should be aware that notwithstanding any other provision of law, no person shall be subject to a penalty for failing to comply with a collection of information if it does not display a currently valid OMB control number.					
1. REPORT DATE 2010		2. REPORT TYPE		3. DATES COVERED 00-00-2010 to 00-00-2010	
4. TITLE AND SUBTITLE Effects of magnetism and doping on the electron-phonon coupling in BaFe2As2			5a. CONTRACT NUMBER		
			5b. GRANT NUMBER		
			5c. PROGRAM ELEMENT NUMBER		
6. AUTHOR(S)			5d. PROJECT NUMBER		
			5e. TASK NUMBER		
			5f. WORK UNIT NUMBER		
7. PERFORMING ORGANIZATION NAME(S) AND ADDRESS(ES) Max-Planck-Institut für Festkörperforschung, Heisenbergstraße 1, D-70569 Stuttgart, Germany, ,			8. PERFORMING ORGANIZATION REPORT NUMBER		
9. SPONSORING/MONITORING AGENCY NAME(S) AND ADDRESS(ES)			10. SPONSOR/MONITOR'S ACRONYM(S)		
			11. SPONSOR/MONITOR'S REPORT NUMBER(S)		
12. DISTRIBUTION/AVAILABILITY STATEMENT Approved for public release; distribution unlimited					
13. SUPPLEMENTARY NOTES					
14. ABSTRACT					
15. SUBJECT TERMS					
16. SECURITY CLASSIFICATION OF:			17. LIMITATION OF ABSTRACT Same as Report (SAR)	18. NUMBER OF PAGES 5	19a. NAME OF RESPONSIBLE PERSON
a. REPORT unclassified	b. ABSTRACT unclassified	c. THIS PAGE unclassified			

In order to disentangle the structural and magnetic effects, we used the high-temperature tetragonal structure^{14,15} in all our calculations. In order to estimate the effect of the SDW ordering vector on the $e-ph$ properties, along with the NM calculations, we have considered two different AFM patterns: the checkerboard one (AFMc), in which the nearest neighbor Fe spins are antiparallel, and the experimentally observed one (AFM stripe, AFMs), in which spins are aligned (anti)ferromagnetically along the $(y)x$ edge of the square Fe planes. The stabilization energies with respect to the NM solutions are 90 meV and 130 meV/Fe atom, respectively.

All calculations were performed in the generalized gradient approximation¹⁶ using plane-waves¹⁷ and ultra-soft pseudopotentials¹⁸. We employed a cut-off of 40 (480) Ryd for the wave-functions (charge densities). The electronic integration was performed over an 8^3 \mathbf{k} -mesh with a 0.01 Ry Hermitian-Gaussian smearing in the NM and AFMc case, while for the AFMs case we used a $8 \times 4 \times 8$ \mathbf{k} -mesh with a 0.01 Ryd Hermitian-Gaussian smearing. Finer grids (20^3 and $20 \times 10 \times 20$) were used for evaluating the densities of states (DOS) and the phonon linewidths. Dynamical matrices and $e-ph$ linewidths were calculated on 4^3 , NM and AFMc case, and 2^3 , AFMs case, uniform grids in \mathbf{q} -space. Phonon frequencies throughout the Brillouin Zone were obtained by Fourier interpolation. The (perturbed) potentials and charge densities, as well as the phonon frequencies, were calculated self-consistently at zero doping ($\delta = 0$); the effect of doping on the $e-ph$ coupling was then estimated using the rigid-band approximation.

The band structures at $\delta = 0$ (not shown) agree with previous calculations.^{11,19} The corresponding magnetic moments and densities of states (DOS) at the Fermi level are reported in table I.²⁰ The phonon dispersion for NM, AFMc, and AFMs cases are shown in the left panels of Fig. 1; the remaining panels show the (partial) densities of states and Eliashberg functions. Our results agree with previous calculations in the same crystallographic structures (adding orthorhombicity additionally changes phonon dispersions, see Refs. 8,9). Magnetism has the biggest effect on phonon modes that involve Fe-As vibrations; there is a pronounced softening of a branch originally located at ~ 25 meV along the $\Gamma-Z$ line in the NM calculation, down to ~ 20 meV in both AFMc and AFMs calculations. This branch corresponds to out-of-plane vibrations of the As atoms. The in-plane Fe-As modes at low and high energy are sensitive not only to the size, but also to the pattern, of the magnetic moment. Indeed, when the order is AFMs, Fe vibrations along the AFM direction harden, whereas those along the FM direction soften, while for the As vibrations it is the opposite.

The shift of phonon frequencies in the AFM calculations has often been considered an indication of an enhanced $e-ph$ coupling in the magnetic phase,^{12,24} but no explicit calculations of the $e-ph$ coupling constant

in the magnetic case have been reported so far. In this work, we have calculated from first principles the same-

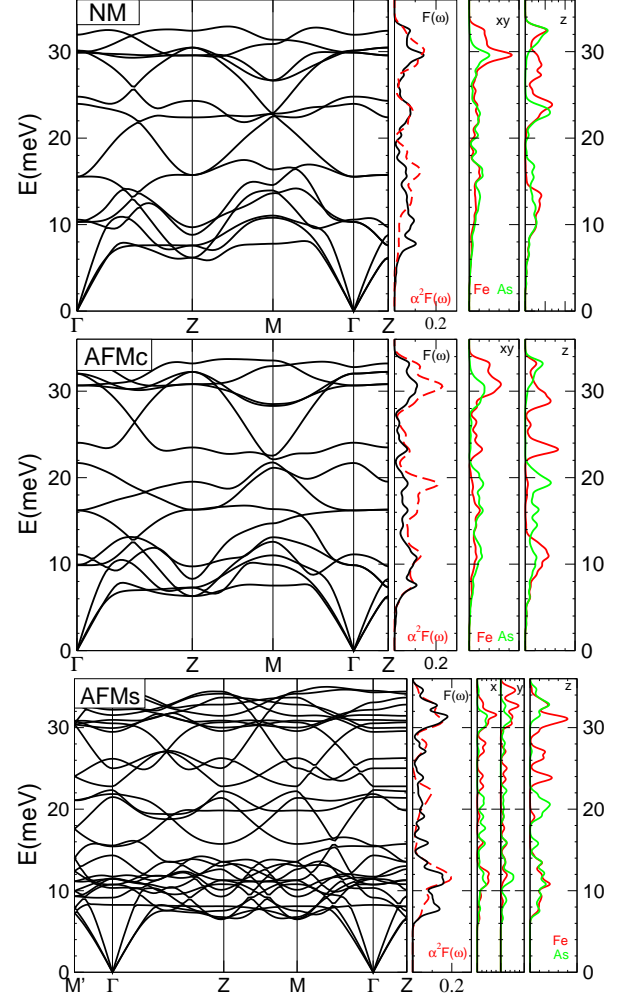


FIG. 1: (color online) Phonon properties of undoped BaFe_2As_2 , for different magnetic patterns: non-magnetic (NM), AFM checkerboard (AFMc) and AFM stripe (AFMs). From left to right: the phonon dispersions; the total phonon densities of states, $F(\omega)$ (red, dashed), and Eliashberg function, $\alpha^2 F(\omega)$ (black, solid); partial contributions of Fe (red, dark) and As (green, light) ions to the total $F(\omega)$, projected onto Cartesian axes (the Ba contribution is limited to $\omega \leq 10$ meV, and not affected by magnetic order). The dispersions are shown in the same Brillouin zone for the three patterns. The \mathbf{k} -points are selected so that they are physically the same in all three structures; the magnetic structure makes the two $\Gamma-M$ directions inequivalent in the AFMs; the spins are aligned AFM(FM) in the $x(y)$ direction. In this coordinate system, the points are: $\Gamma = (0,0,0)$; $Z = (0,0,\pi/c)$ or $(\pi/a,\pi/a,0)$; $M = (\pi/a,0,0)$; $M' = (0,\pi/2a,0)$, where a is the length of the shortest Fe-Fe bond and c is the Fe-Fe interlayer distance.

spin component of the Eliashberg spectral function:

$$\alpha^2 F_{\sigma\sigma}(\omega) = \frac{1}{N_{\sigma}(0)N_k} \sum_{\mathbf{k}, \mathbf{q}, \nu} |g_{\mathbf{k}, \mathbf{k}+\mathbf{q}}^{\nu, \sigma}|^2 \times \delta(\varepsilon_{\mathbf{k}}^{\sigma}) \delta(\varepsilon_{\mathbf{k}+\mathbf{q}}^{\sigma}) \delta(\omega - \omega_{\mathbf{q}}^{\nu}), \quad (1)$$

$$g_{\mathbf{k}n, \mathbf{k}+\mathbf{q}m}^{\nu, \sigma} = \langle \mathbf{k}^{\sigma} n | \delta V_{\sigma} / \delta e_{\mathbf{q}\nu} | \mathbf{k} + \mathbf{q}^{\sigma} m \rangle / \sqrt{2\omega_{\mathbf{q}\nu}}.$$

Here, N_k is the number of \mathbf{k} -points used in the summation, $N_{\sigma}(0)$ is the density of states per spin at the Fermi level, and $\omega_{\mathbf{q}}^{\nu}$ are the phonon frequencies. The $e-ph$ matrix element $g_{\mathbf{k}n, \mathbf{k}+\mathbf{q}m}^{\nu, \sigma}$ is defined by the variation of the self-consistent crystal potential V_{σ} for the spin σ with respect to a frozen phonon displacement according to the phonon eigenvector $e_{\mathbf{q}\nu} = \sum_{A\alpha} M_A \sqrt{2\omega_{\mathbf{q}\nu}} \epsilon_{A\alpha}^{\mathbf{q}\nu} u_{\mathbf{q}A\alpha}$. Here $u_{\mathbf{q}A\alpha}$ is the Fourier transform of the α component of the phonon displacement of the atom A in the unit cell, M_A is the mass of atom A and $\epsilon_{A\alpha}^{\mathbf{q}\nu}$ are $A\alpha$ components of $\mathbf{q}\nu$ phonon eigenvector normalized in the unit cell. The first inverse moment of $\alpha^2 F(\omega)$ gives the frequency-dependent $e-ph$ coupling constant:

$$\lambda_{\sigma\sigma}(\omega) = 2 \int_0^{\omega} d\Omega \alpha^2 F_{\sigma\sigma}(\Omega) / \Omega. \quad (2)$$

The total $e-ph$ coupling constant $\lambda_{\sigma\sigma} = \lambda_{\sigma\sigma}(\omega = \infty)$ is 0.18, 0.33 and 0.18 for NM, AFMc and AFMs, respectively.

The three calculations in Fig. 1 have different phonon spectra $\omega_{\mathbf{q}}^{\nu}$, different self-consistent crystal potentials V_{σ} , and different one-electron wave-functions $|\mathbf{k}n\rangle$ and eigenenergies $\varepsilon_{\mathbf{k}}^{\sigma}$, which all determine the value of λ in Eqs. 1-2. In order to understand which of these factors dominates the $e-ph$ coupling, we start for simplicity from the so-called Hopfield formula for the $e-ph$ coupling constant:

$$\lambda_{\sigma\sigma} = \frac{N_{\sigma}(0)D^2}{M\omega^2}, \quad (3)$$

where D is the deformation potential, which is a measure of the average $e-ph$ interaction, and $M\omega^2$ is a characteristic force constant, which we assume depends weakly on the magnetic order. We can then use the ratio $\lambda_{\sigma\sigma}/N_{\sigma}(0)$ to obtain an estimate for the average change in the $e-ph$ interaction due to magnetism; going from NM to AFMc (AFMs), this ratio, and hence D^2 , increases by $\sim 50\%$, from 0.15 to 0.24 (0.26) - see table I. A comparison of Eq. 1 and Eq. 3 shows that the increase in D can be caused either by an increase in the derivative of the DFT potential V_{σ} with respect to displacement, or by a difference in the one-electron wavefunctions, used to evaluate its average over the Fermi surface. In order to disentangle these two effects, we performed a mixed calculation (PM1), in which we combined the NM eigenvalues and wavefunctions, as well as the phonon frequencies, with the AFMc potential variations in the Eq. 1. In the top panel of Fig. 2, we compare the resulting Eliashberg function $\alpha^2 F(\omega)$ with the NM one; the total phonon DOS

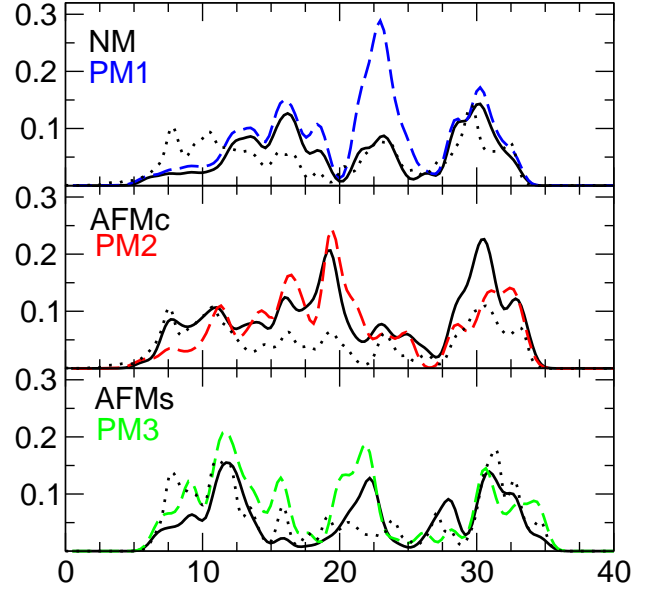


FIG. 2: (color online :) The Eliashberg functions $\alpha^2 F(\omega)$ for the non-magnetic (NM, top, black solid line), anti-ferromagnetic (AFM, middle and bottom, black solid lines) and model paramagnetic calculations, as described in the text, (PM1-3, colored dashed lines). The corresponding phonon densities of states, in arbitrary units, are shown in each panel by the dotted lines.

$F(\omega)$ is also shown as dotted lines. The effect of using the AFM potential is an increased coupling of electrons to phonons with frequencies $\omega \sim 20 - 25$ meV, while other modes are largely unaffected. This increases λ from 0.18 (NM) to 0.27 (PM1). The middle and lower panel of Fig. 2 show two calculations, PM2 and PM3, which use NM one-electron wave functions, and AFMc and AFMs phonon frequencies and crystal potentials, respectively. A comparison of the $\alpha^2 F(\omega)$ with the phonon densities of states shows that, also in these cases, there is an increased coupling to phonons around 20 meV, both in AFM and PM. The λ 's, reported in table I, are 0.27 and 0.31, for PM2 and PM3 respectively. From the comparison of PM1 and PM2, we conclude that the effect of the phonon frequency is negligible, while the $\sim 10\%$ spread of values between PM2 and PM3 gives an indication of the effect of the short range AFM correlations on λ . Finally, we find that the values of $\lambda_{\sigma\sigma}/N_{\sigma}(0)$ in the PM calculations are in line with the AFM ones, indicating that, at $\delta = 0$, the states at E_F have a comparable, weak coupling to phonons, for both NM and AFM orders.

These model calculations, which combine the AFM potentials and phonons and the NM wavefunctions and Fermi surfaces, represent the best approximation, at LDA level, of the real *paramagnetic* (PM) state of superconducting, doped, BaFe_2As_2 which is characterized by local, disordered magnetic moments.²¹ In the following, we will use them to estimate an upper bound for the $e-ph$ coupling in the *doped* BaFe_2As_2 .

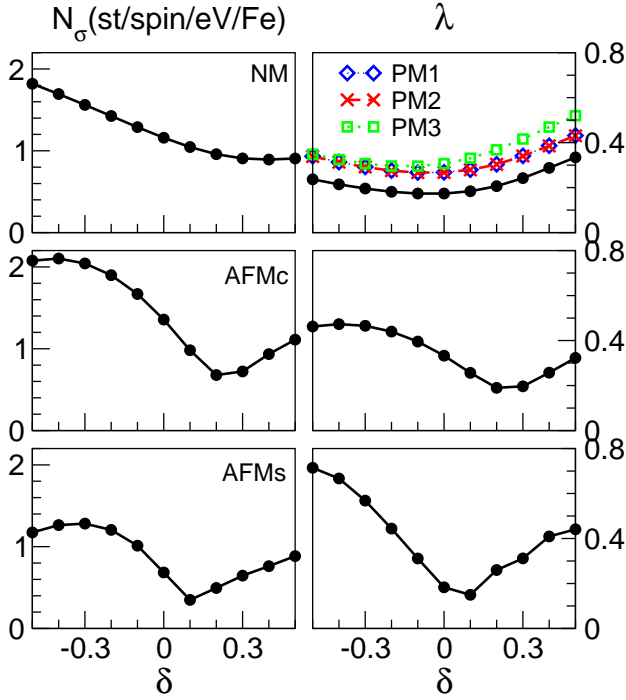


FIG. 3: (color online) Effect of doping on the $e-ph$ coupling of BaFe_2As_2 , in the rigid-band model. $\pm\delta$ is the number of excess electrons/holes per Fe atom. The left panel shows the density of states at E_F , in states/spin eV Fe atom. The right panel shows the same-spin coupling constant $\lambda = \lambda_{\sigma\sigma}$. $N_\sigma(0)$ is the same for NM and all three (see text) PM calculations, as described in text.

In Fig. 3, we show the density of states at the Fermi level $N_\sigma(0)$ (left) and $\lambda_{\sigma\sigma}$ (right) as a function of doping δ for NM, AFMc, AFMs, and PM orders, from a rigid-band calculation; δ is defined as the number of excess electrons (holes) per Fe atom. NM and PM calculations have the same $N_\sigma(0)$, which decreases monotonically as a function of doping, while $\lambda_{\sigma\sigma}$ is roughly symmetric around $\delta = 0$.

This indicates that, in Eqs. 1-3, the effect of the matrix element dominates over that of the DOS. In the AFM calculations, the shape of the $\lambda_{\sigma\sigma}$ curve follows more closely that of $N_\sigma(0)$, with a minimum at $\delta \sim 0.1 - 0.2$, and a maximum $\lambda_{\sigma\sigma} = 0.8$ for AFMs at $\delta = -0.5$, corresponding to KFe_2As_2 . However, the use of the rigid-band approximation is questionable at these high dopings, and in the following we limit our analysis to a smaller range of $\delta = \pm 0.25$, where the error in λ connected to the rigid-band approximation is $\lesssim 20\%$.²²

We can summarize the results of Fig. 3, by saying that, for $|\delta| < 0.25$, the upper bound for the $e-ph$ coupling in paramagnetic, superconducting $\text{BaFe}_2\text{As}_2 + 2\delta$ is $\lambda_{\sigma\sigma} \lesssim 0.35$. The enhancement in λ results from a $\sim 50\%$ increase in the $e-ph$ matrix elements, due to static magnetism, which is independent on doping, and a symmetric increase of the matrix element for $\delta \neq 0$, which does not follow the shape of the electronic DOS.

The value $\lambda_{\sigma\sigma} = 0.35$, which includes magnetism and doping, is almost a factor of two larger than that estimated in early non-magnetic calculations for the undoped compounds,^{1,2} and close to a recent experimental estimate of λ from a kink in photoemission spectra.⁴

What are the consequences of this result? Of course, it cannot explain a T_c of 38 K, which confirms that superconductivity in this and other Fe-based superconductors is most likely due to electronic (magnetic) degrees of freedom.^{2,23} However, in Fe pnictides, studies of the superconducting gap in realistic models with AFM spin fluctuations show that solutions with and without gap nodes are almost degenerate, so that even a relatively low $e-ph$ coupling constant can help select either of them, by enhancing/suppressing the pairing in the relevant channel.^{24,25}

Acknowledgements: L.B. wishes to thank O.K. Andersen for encouragement, support, and advice. Part of the calculations were performed at the IDRIS superconducting center.

- ¹ L. Boeri, *et al.*, Rev. Lett. **101**, 026403 (2008) and Physica C **469**, 628 (2009).
- ² I. I. Mazin, *et al.*, **101**, 057003 (2008).
- ³ R. H. Liu, *et al.*, Nature **459**, 64 (2009); P. M. Shirage, *et al.*, Phys. Rev. Lett. **103**, 257003 (2009).
- ⁴ A. A. Kordyuk, *et al.*, cond-mat/1002.3149.
- ⁵ M. Rahlenbeck, *et al.*, Phys. Rev. B **80**, 064509 (2009).
- ⁶ K.-Y. Choi, *et al.*, cond-mat/0908.4364.
- ⁷ I. I. Mazin, *et al.*, Phys. Rev. B **78**, 085104 (2008).
- ⁸ T. Yildirim, Phys. Rev. Lett. **102**, 037003 (2009) and Physica C **469**, 425 (2009).
- ⁹ M. Zbiri, *et al.*, Phys. Rev. B **79**, 064511 (2009); S.E. Hahn *et al.*, Phys. Rev. B **79**, 220511(R) (2009).
- ¹⁰ D. Reznik, *et al.*, Phys. Rev. B **80**, 214534 (2009).
- ¹¹ I. I. Mazin, M. D. Johannes, Nat. Phys. **5**, 141 (2008).
- ¹² M. D. Johannes and I. I. Mazin, Phys. Rev. B **79**, 220510 (2009).

- ¹³ F. Yndurain and J. M. Soler, Phys. Rev. B **79**, 134506 (2009).
- ¹⁴ S. Baroni, *et al.*, Rev. Mod. Phys. **73**, 515, (2001).
- ¹⁵ M. Rotter, *et al.*, Phys. Rev. B **78**, 020503 (2008).
- ¹⁶ The lattice constants, as well as the internal coordinate of the As atoms, are set to the experimental values: $a = 3.96\text{\AA}$, $c = 13.02\text{\AA}$, $z_{\text{As}} = 0.3545$.
- ¹⁷ J. P. Perdew, K. Burke, and M. Ernzerhof, Phys. Rev. Lett. **78**, 1396 (1997).
- ¹⁸ P. Giannozzi *et al.*, <http://www.quantum-espresso.org>.
- ¹⁹ D. Vanderbilt, Phys. Rev. B **41**, R7892 (1990).
- ²⁰ D. J. Singh, Phys. Rev. B **78**, 094511 (2008).
- ²¹ Notice that the magnetic moment reported in table I is actually the integral of the absolute value of the magnetization over the cell, and therefore larger than the moment inside the Fe muffin-tin sphere, usually quoted in LAPW calculations.

²¹ P. Hansmann, *et al.*, cond-mat/1003.2162.

²² The accuracy of the rigid band approximation is difficult to access quantitatively, given that the e-ph coupling is sensitive not only to the band structure, but also to the magnetic moments and the deformation potential. However, we have verified that for the doping $|\delta| = 25\%$ the Density of states (DOS) of the entire Fe-derived band, calculated in the corresponding supercells, and in the virtual crystal approximation, remains rather close (*i.e.* $\pm 10\%$) to

the rigid band DOS, therefore we consider application of the rigid band approximation in this interval to be meaningful.

²³ K. Kuroki, *et al.*, Phys. Rev. Lett. **101**, 087004 (2008);

²⁴ I.I. Mazin and J. Schmalian, Physica C **469**, 614 (2009).

²⁵ K. Kuroki *et al.*, Phys. Rev. B **79**, 224511 (2009); A. F. Kemper, *et al.*, cond-mat/1003.2777; R. Thomale *et al.*, cond-mat/1002.3599.